Regular Article

PHYSICAL CHEMISTRY RESEARCH
Published by the
Iranian Chemical Society
www.physchemres.org
info@physchemres.org

Phys. Chem. Res., Vol. 12, No. 3, 783-800, September 2024
DOI: 10.22036/pcr.2024.425179.2450

Study of the Anticancer Potential of Cannabidiol Using Computational Methods

S. Aissaoui[a], H. Hajjia[b], H. Zaki[a,*], M. Alaqarbeh[c], S. Chtita[d], T. Lakhlifi[b], M.A. Ajana[b] and M. Bouachrine[a,b]

[a]*Biotechnology, Bioresources, and Bioinformatics Laboratory, Higher School of Technology-Khenifra, University of Sultan My Slimane, PB 170, Khenifra 54000 Morocco*

[b]*Molecular Chemistry and Natural Substances Laboratory, department of chemistry, Faculty of Science, My Ismail University, Meknes, Morocco*

[c]*Laboratory of Chemistry-Biology Applied, National Agricultural Research Center, Al Baqa 19381, Jordan*

[d]*Laboratory of Analytical and Molecular Chemistry, Faculty of Sciences Ben M'Sik, Hassan II University of Casablanca, Casablanca7955, Morocco*

(Received 18 September 2023, Accepted 28 January 2024)

In this work, molecular docking was performed to evaluate the anticancer activities of cannabidiol on various targeted proteins. Interactions and significant binding energy prove that cannabidiol can be synthesized and tested as a potent drug that treats all types of human cancer safely. The data obtained highlight the key amino acids involved in the ligand/protein interactions and show that the designed cannabidiol-bound complexes exhibited the best confirmation in the binding site. In addition, a DFT optimization of the geometry and orbital frontier analysis was performed to describe the chemical reactivity of the studied molecule. A pharmacokinetic and bioavailability study in the body was performed by ADMET proprietors. The results of the molecular docking indicate that cannabinol can be tested as a potent drug to treat human cancer, given its interactions and significant binding energy up to -8.6 kcal mol^{-1} with FAAH protein.

Keywords: Cannabidiol, Anticancer, Molecular docking, DFT, ADMET

INTRODUCTION

The medicinal use of *Cannabis sativa* has a long history dating back to ancient times in China because it contains more than 100 different chemical compounds and represents a great academic and pharmaceutical interest [1-2]. *Cannabis sativa* is considered the main source of phytocannabinoids, and more than 100 different types of secondary metabolized active compounds are known as tetrahydrocannabinol (THC) and cannabidiol (CBD) [3]. THC is known for its psychoactive properties, while CBD is not psychoactive but has anti-tumor activity [4]. Also, CBD has antioxidant and anti-inflammatory properties [5].

CBD's pharmacological effects are due to its ability to mimic endogenous cannabinoids (endocannabinoids), which are mediated by specific cannabinoid receptors [6]. In addition, CBD acts on multiple targets other than CB1/CB2, where it can bind to other transmembrane proteins, including the orphan G protein-coupled receptor 55 (GPR55), peroxisome proliferator-activated receptors (PPARs), and transient receptor potential vanilloid channels (TRPV1/TRPV2) [7]. Also, CBD induces apoptosis by modulating numerous pro- and anti-apoptotic proteins and reducing tumor growth [8]. In addition to its ability to inhibit several cancer factors, including 5-HT1A, Becl1, COX-2, DR5, EGF, FAAH, ICAM-1, NOS3, NOXA, PAI-1, RERK, and TIMP-1 [9,10].

*Corresponding author. E-mail: mmezakihanane@gmail.com

The 5-HT1A receptor has been widely implicated in carcinogenesis and thus has been implicated in many types of human tumors, including prostate, bladder, small cell lung, colon, and cholangiocarcinoma [11]. 5-HT1A receptor antagonists have been shown to block the activities of 5HT, PI3K/AKT, and MAPK but mediate pathways of JAK/STAT antitumor immune responses through various receptors [12]. The Beclin-1 protein is essential for the induction of autophagy [13]. CB1 and CB2 exert antitumor effects by suppressing the NF-κB signaling pathway and increasing apoptotic cell death [14]. Overexpression of COX-2 increases angiogenesis, migration, invasiveness, and tumor-induced immunosuppression and prevents apoptosis [15], and DR5-target can induce apoptosis [16]. Epidermal growth factor receptor (EGFR) activity promotes tumor growth, invasion, and metastasis. This justifies efforts to inhibit EGFR signaling [17]. FAAH inhibitors in several cancer cell lines inhibit growth and proliferation, reduce migration, and have invasion properties [18]. GPR55 is involved in oncogenic processes such as cell proliferation, differentiation, migration, invasion, and metastasis, which are altered in some cancer cells. Overexpression or high expression of GPR55 is correlated with cancer aggressiveness [19]. ICAM-1 can promote metastasis, stimulate proliferation, angiogenesis, and invasion, and combat apoptosis in cancer cells [20].

ICAM-1 expression downregulation can inhibit cell migration and invasion [21], and NOS3 is critical in autophagic cell death induced by CBD production [22]. Noxa is important in regulating apoptosis in CBD-induced cells, induces cytotoxicity through inhibition of PAI-1 expression, decreases proliferation, migration, and invasive potential of lung cancer cells, and suppresses angiogenesis and metastasis formation [23,24].

PERK plays a vital role in the induction of apoptosis mediated by CBD [25]. It has been reported that PPARG can promote cancer progression by maintaining redox balance and promoting cell survival; blocking PPARG function leads to apoptosis [26]. TIMP-1 activity is observed in various tumor tissues as an important indicator of invasion and metastasis [27]. TRPV1 reduces cell growth and increases apoptosis, and TRPV2 expression increases cancer aggressiveness by promoting migration [28,29].

All previous factors interacting with CBD could be a potentially useful therapeutic option to improve chemosensitivity and cytotoxic effects on cancer cells and reduce cancer spread [29]. Previous studies have shown that CBD has a very complex mechanism of action as an anti-cancer agent [30]. However, despite a large number of *in vivo* and *in vitro* studies, there is still a need for more research to prove that CBD is synthesized and tested as a powerful drug that safely treats different types of human cancer [31].

As shown in Fig. 1, CBD has a very complex mechanism of action as an anti-cancer agent that safely treats different types of human cancer.

The current study pinpoints the interaction of cannabidiol (CBD) with the receptors responsible for anti-tumor action based on theoretical methods using the density function theory (DFT), molecular docking, and *in silico* ADMET proprieties. The optimized geometries were achieved by DFT method. The reactivity calculations predicted the interactions in the ligand-protein complex and their molecular boundary orbital analysis sites, which helped obtain the best molecular docking results. ADME/toxicity study was conducted to predict the bioavailability of cannabidiol.

MATERIAL AND METHODS

Density fFunction Theory (DFT) Calculation

Gaussian 09 and GaussView 5 [32] were used to calculate the optimal geometrical parameters of the target molecules using the density functional theory (DFT) approach at the B3LYP/6-31G++ level with Gaussian 09 and GaussView 5. In this approach, the B3LYP functional, a hybrid functional combining the three-parameter Becke exchange (B3) and Lee-Yang-Parr correlation (LYP) functions, was used to determine the properties of cannabidiol and its electronic structure, based on 6-31G++ The molecules were imported into Gaussian 09 via GaussView 5.

The software then performed energy optimization calculations, where atom positions were adjusted to find the most stable configuration. These calculations provide geometrical information such as bond lengths and indications of electronic properties, such as the most stable and least energetic configuration, and the energies of the frontier orbitals. The most occupied molecular orbital (HOMO) and the least occupied molecular orbital (LUMO) - and other parameters generated from these two energies and the molecular electrostatic potential (MESP).

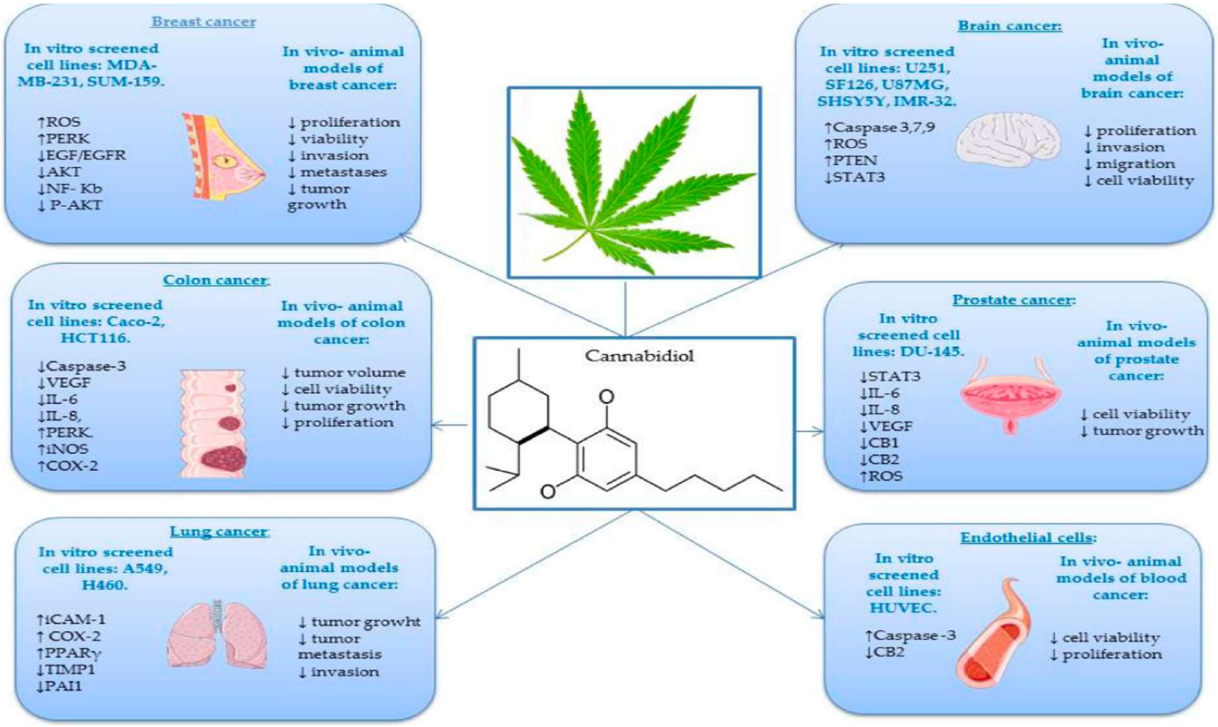

Fig. 1. Role of CBD among various cancer models [10].

Table 1. Overview of Proteins Used

Receptor type	Pdb ID	Bound ligand	Importance	Ref.
5-HT1A	7 e2z	Antagonist	Antitumor immune responses	[12]
Becl1	3q8t	Activator	Induction of autophagy	[13]
CB1	5tgz	Antagonist	Induction of apoptosis	[14]
CB2	2hff	Inverse agonist	Induction of apoptosis	[14]
COX-2	1pxx	Inhibitor	Reduce invasion	[15]
DR5	4i9x	Against	Induce apoptosis	[16]
EGF	1ivo	Agonist	Reduce invasion	[17]
FAAH	2wap	Inhibitor	R invasion	[18]
GPR55	4n6h	Antagonist	Reduce invasion	[19]
ICAM-1	1iam	Activator	Reduce invasion	[20]
NOS3	1m7z	Inhibitor	Autophagic	[22]
NOXA	3mqp	Activator	Regulating apoptosis	[23]
PAI-1	7aqf	Inhibitor	Decreases proliferation	[24]
PERK	4g31	Inducer	Induction of apoptosis	[25]
PPARɣ	5ycp	Agonist	Reduce invasion	[26]
TIMP-1	1d2b	Inhibitor	Increases apoptosis	[27]
TRV1	7lqz	Agonist	Form metastases	[28]
TRV2	6u8a	Agonist	Reduce migration	[29]

Docking Molecular

Protein preparation. The cancer target proteins were downloaded in "pdb" format from the RCSB Protein Data Bank (PDB) database (https://www.rcsb.org) and were visualized using BIOVIA Discovery Studio [33]. Then, the protein was prepared and saved in PDBQT format in AutoDock workspace 4.2.6. in which polar hydrogen atoms and Kollman and Gasteiger charges were added for the protein [34]. Table 1 displays the types of target studies, along with their corresponding PDB codes, the type of binding with the molecule, and their importance in anti-cancer activity.

Ligands preparation. The DFT-optimized structure of cannabidiol (CBD) was imported and prepared in AutoDock workspace 4.2.6 for molecular docking simulation. Ligand preparation involves converting the ligand into the PDBQT format specifically required by AutoDock for docking. This format contains crucial information such as the partial charges and atom types required for accurate docking simulation.

Visualization of protein-ligand interaction. The Autogrid algorithm in MGL Tools 1.5.6 was used to determine the potential size of the binding pocket between the receptor and cannabidiol. By setting the parameters to 8 binding modes and completeness of 8, grid maps were generated using a size of 40 Å in all Cartesian directions. The binding pocket was defined using XYZ coordinates as shown in Table 2. Computational docking was performed with AutoDockVina software, and the Biovia Discovery Studio viewer was used to analyze docked conformations on the basis of established interactions [35].

Table 2. Overview of (XYZ) Grid Center Coordinates Used

Pdb ID	x	y	z
7 e2z	93.694	73.002	87.111
3q8t	-59.211	-19.557	42.039
5tgz	43.637	27.469	318.530
2hff	-11.690	21.446	9.996
1pxx	69.156	36.960	34.659
4i9x	-4.491	12.415	48.441
1ivo	43.302	54.846	66.402
2wap	-6.748	27.359	37.499
4n6h	-5.910	69.366	70.805
1iam	37.909	79.263	12.440
1m7z	5.2869	43.300	13.035
3mqp	9.957	17.951	1.294
7aqf	34.166	9.525	23.511
4g31	-33.089	8.808	1.401
5ycp	35.1820	32.288	11.502
1d2b	-11.129	1.782	2.940
7lqz	170.831	105.917	107.590
6u8a	160.968	142.496	172.069

Physiochemical and Pharmacokinetic Evaluation

Prediction of the pharmacokinetic properties of cannabidiol is essential to determine the absorption, distribution, metabolism, excretion, and toxicity of the active candidate molecules currently being studied for potential cancer treatment and it was done using SwissADME (http://www.swissadme.ch/).

RESULTS AND DISCUSSION

Optimized Molecular Geometry

Experimental information about the geometric properties of cannabidiol is insufficient in the literature. Theoretical calculation of the geometrical parameters of cannabidiol before optimization by DFT methods shows that cannabidiol has rings with an average C-C bond length of 1.550 Å, while the average C=C bond length is 1.386 Å where the typical C=C bond length is 1.346 Å and the typical distances between the C-C and C-H atoms for the substituted methyl are 1.519 Å and 1.110 Å, respectively. The H-C-H angle of the methyl group is approximately 109°, and the alkene creates an angle with the neighboring carbon of about 123° of sp3 hybrid carbon forms an angle of about 120° with the C-C-C in the aromatic ring. When comparing the results in Table 3 with the CBD binding lengths before optimization by DFT, there is no difference.

The cannabinol CBD molecule includes two rings. metabenzenediol and cyclohexene (Fig. 2). The chemical activity of cannabidiol (CBD) could result from the attachment of the hydroxyl radical teams to the C-1 and C-3 atoms of the benzene. Similarly. the alkyl radical fixed to the C-16 atom of the cyclohexene and pentyl to the C-5 atom of the aromatic ring can also contribute to the reactional activity of the molecule considered.

Table 3. Calculated Bond Lengths of Cannabinol Molecule Using DFT Calculation

Bond lengths (Å)					
C1-C6	1.384	C11-C12	1.531	C17-C18	1.528
C1-O1	1.360	O7-H28	1.012	C18-H44	1.111
C1-C2	1.386	08-H29	1.012	C18-H45	1.111
C2-C14	1.536	C12-H36	1.111	C18-C19	1.526
C2-C3	1.389	C12-H37	1.111	C19-H25	1.115
C3-08	1.360	C12-C13	1.530	C19-C21	1.522
C3-C4	1.387	C13-H40	1.111	C21-C22	1.510
C4-H26	1.111	C13-H38	1.111	C21-C20	1.342
C4-C5	1.386	C13-H39	1.111	C20-H46	1.111
C5-C6	1.386	C14-H24	1.114	C20-H47	1.111
C5-C9	1.519	C14-C19	1.550	C22-H49	1.111
C9-H31	1.111	C14-C15	1.531	C22-H48	1.111
C9-H30	1.111	C15-C16	1.346	C22-H50	1.111
C9-C10	1.535	C15-H41	1.111	C23-H53	1.111
C10-H32	1.111	C16-C23	1.509	C23-H51	1.111
C10-H33	1.111	C16-C17	1.519	C23-H52	1.111
C10-H35	1.111	C17-H42	1.111		
C11-H34	1.111	C17-H43	1.111		

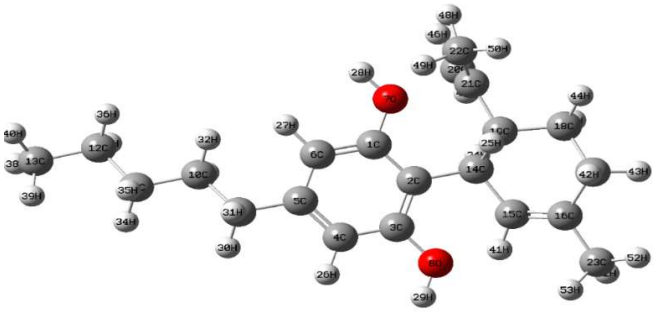

Fig. 2. Optimized geometry of cannabidiol optimized at the DFT/B3LYP/6-311++G(d.p) level.

Frontier molecular orbital analysis HOMO-LUMO

HOMO and LUMO energies provide kinetic stability, chemical analysis, and band gap approximation [36]. Equations ((1)-(7)) are used to calculate the following quantum mechanical descriptors in Table 4: electrophilicity index (ω), chemical softness (σ) and hardness (η), electronegativity (χ), electronic affinity (EA), and ionization potential (IP) [37].

As shown in Table 4 calculating, the electronic descriptions of cannabidiol (CBD) provide the essential information needed to understand its potential as a cancer treatment candidate. The LUMO's energy of 0.01 eV suggests that CBD may be an important electron acceptor in interactions with the targets involved in the anticancer response. Furthermore, the HOMO has a lower energy of -0,134 eV, suggesting a strong electron-donation capacity [38]. The band gap energy E and the negative molecular chemical potential value of the cannabidiol molecule confirm that the molecule has a stable structure, electronic stability can also influence the duration of interactions [39]. A higher nucleophilic reactivity indicated by the lower value of the electronic affinity and electrophilicity index [40], may contribute to the development of interactions with functionally distinct groups within proteins. The higher values of durability and lower values of softness confirm that the durability of the molecule is higher and stability is one of the main characteristics of molecules that can be very reactive agents in anti-cancer activity [41]. According to these findings, the charge transition process is desirable in terms of energy when interacting with proteins.

The first feature found is that LUMO is located on the π and π* orbitals of the benzene ring. and HOMO is on the methyl group structure as shown in Fig. 3.

Energy gap (ΔE_{GAP} (eV))	$\Delta E = E_{LUMO} - E_{HOMO}$	(1)
Electronic affinity (eV)	$EA = -E_{LUMO}$	(2)
Ionization potential (eV)	$IP = -E_{HOMO}$	(3)
Chemical hardness (eV)	$\eta = \frac{\Delta E}{2}$	(4)
Chemical softness (eV)	$\sigma = \frac{1}{\eta}$	(5)
Electronegativity (eV)	$\chi = \frac{(IP + EA)}{2}$	(6)
Electrophilicity index ω (eV)	$\omega = \frac{\chi 2}{2\eta}$	(7)

Table 4. Reports the Values of the Global Molecular Descriptors Calculated for Cannabidiol

$E_{(LUMO)}$ (eV)	$E_{(HOMO)}$ (eV)	ΔE (eV)	IP (eV)	EA (eV)	η (eV)	χ (eV)	ω (eV)	σ (eV)
0.012	-0.134	0.146	-0.012	0.134	0.073	0.060	0.0251	13.63

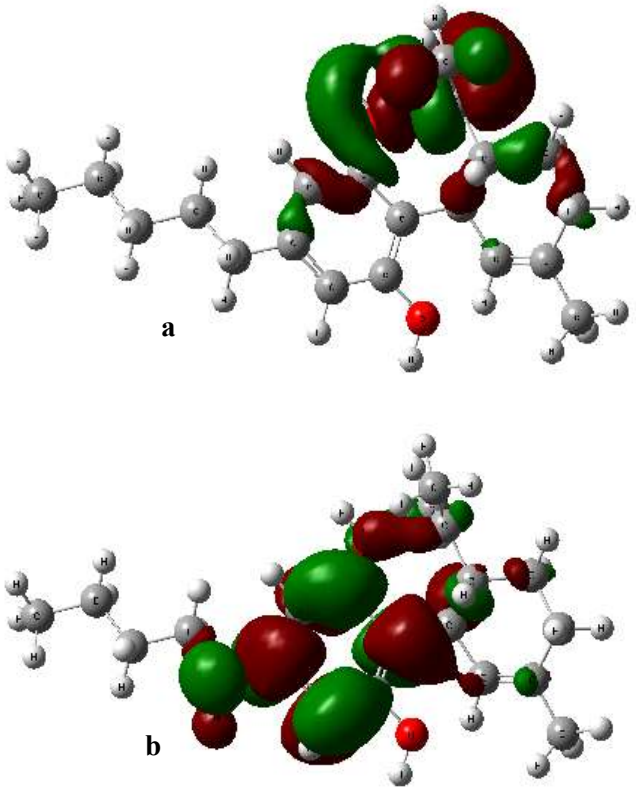

Fig. 3. HOMO (a) and LUMO (b) representation of CBD by DFT/631G method.

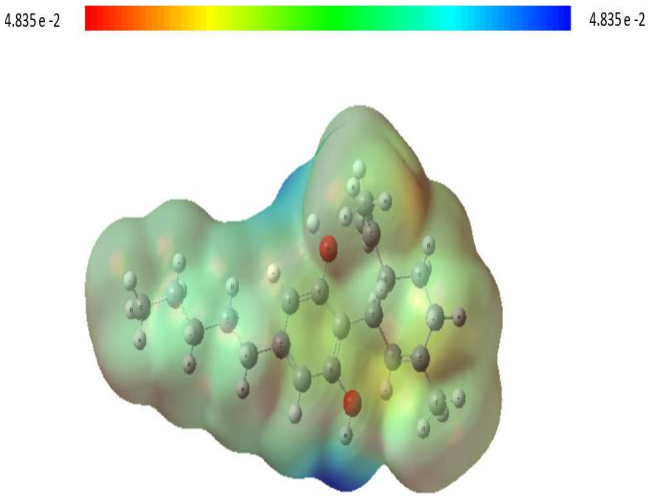

Fig. 4. Molecular electrostatic potential (MEP) surface of the cannabidiol (CBD) molecule.

Molecular Electrostatic Potential (MEP)

The interaction energy between the positive test charge of the molecular system and its charge distribution is known as the molecular electrostatic potential (MEP). It provides essential details on the chemical stability and reactivity of a semi-organic molecule. allowing us to understand its electrophilic and nucleophilic properties.

Figure 4 shows a color scale from red (negative MEP) through white (neutral MEP) to blue (positive MEP). where blue regions indicate a vulnerable site for an electrostatic-type nucleophilic attack and red regions are sites for an electrostatic-type electrophilic attack [42].

The negative electrostatic potential (region colored in red) was observed around the carbon atoms of the phenolic ring of the oxygen atom group. The positive electrostatic potential (region colored in blue) was observed around the methyl group and the hydrogen atoms, this is due to the electronegative oxygen atom attracting electrons from the hydrogen atoms [43] which suggests that cannabidiol's biological activity is essentially due to the presence of the hydroxyl group.

Molecular docking. Binding to 5-HT1A: Imidazole 5-HT1A showed an affinity of -7.4 (kcal mol^{-1}) with CBD. Figure 5 where the hydroxyl group formed a hydrogen bond with the oxygen of amino acids SER316 and MET188 with distances of 2.408 Å and 2.253 Å, respectively. A pi-alkyl interaction between the carbon of the pentyl group and the Imidazole of HIS213 at 5.467 Å while an alkyl interaction was observed for cyclohexenyl group with ALA60 at 5.052 Å.

Binding to Becl1. Figure 6 shows the interaction between CBD and Becl1 with a binding affinity of -5.5 kcal mol^{-1}. The hydrogen bond interaction was formed at the carbonyl group of amino acid ALA215 at 2.167 Å. In contrast, a carbon-hydrogen bond was formed between the oxygen of the hydroxyl group and the carbon of ARG219 at 3.692 Å. A pi-sigma bond was observed at 3.846 Å between the benzene ring and the methyl group of ALA215. Six alkyl interactions were found between the isopropyl group of ARG219 and the cyclohexenyl group of CBD at 4.127 Å and cyclohexene at 4.925 Å and between the pentyl carbon and LEU220 (5.470 Å), LYS212 (5.051 Å), and VAL213 (4.270 Å).

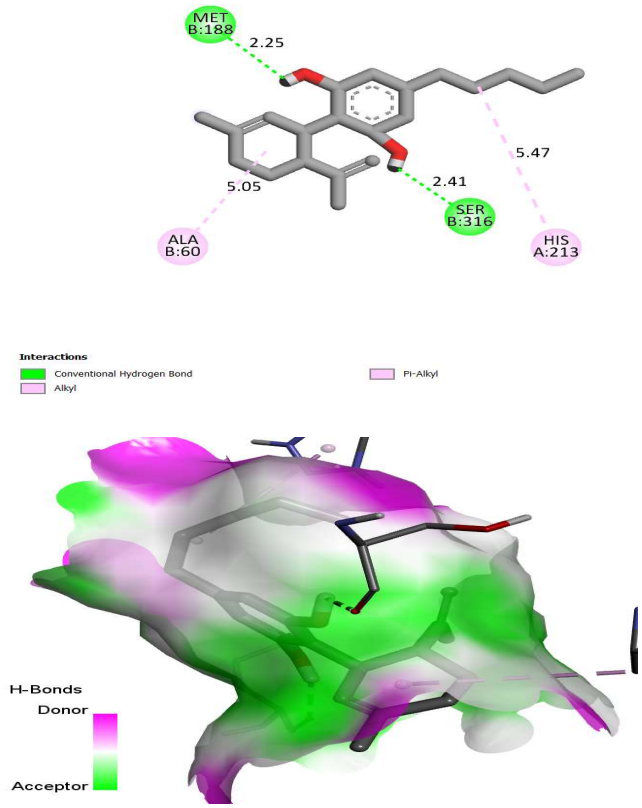

Fig. 5. 3D and 2D docked views of CBD with 5-HT1A Protein.

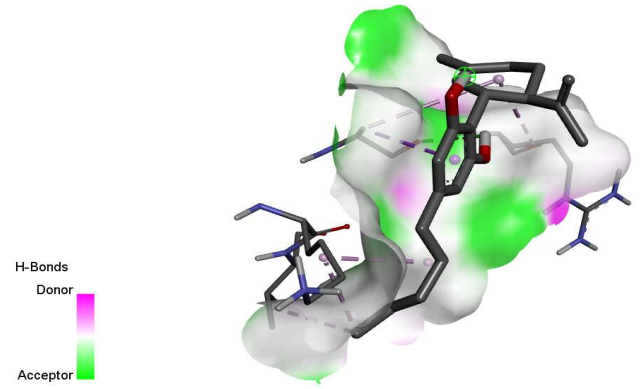

Fig. 6. 3D and 2D docked views of CBD with Becl1 Protein.

Binding to CB1. The binding energy between CBD and CB1 is -6.5 (kcal mol^{-1}) due to hydrogen bonding interaction observed at the hydroxyl group of cannabidiol with the oxygen of SER123 at 2.115 Å. Ten alkyl bonding between cannabidiol and (MET103 at 4.976 Å), (MET103 at 4.384 Å), (MET384 at 5.108 Å), (ILE119 at 4.353 Å), and (MET384 at 4.288 Å). And Pi-Alkyl interaction with (PHE170 at 5.011 Å), (PHE381 at 5.019 Å), (ALA380 at 5.016 Å), and (MET384 at 4.814 Å) (Fig. 7).

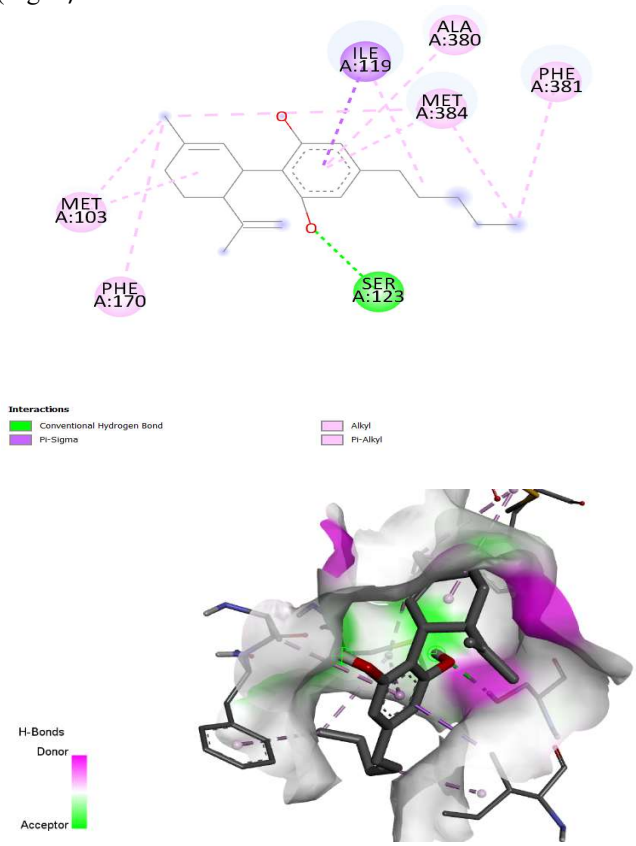

Fig. 7. 3D and 2D docked views of CBD with CB1 Protein.

Binding to CB2. CBD shows binding with CB2 with a binding energy of -6.8 (kcal mol^{-1}) due to the binding affinity between CB2 and CBD is -6.8 (kcal mol^{-1}). The hydroxyl group of CBD forms hydrogen bonds with CB2 and the hydrogen of the amine group of GLU212 at 2.351 Å and the oxygen of PRO119 at 2.073 Å. A Pi-Anion interaction at 2.073 Å between the benzene of CBD and PRO119. In addition, two alkyl bonds exist between (PRO118 at 4.152 Å) and (ARG210 at 4.796 Å) and the carbon of CBD. Two pi-alkyl interactions between the benzene of CBD and ARG210 at 4.834 Å and the benzene PHE208 with the carbon of the methyl group CBD at 4.927 Å. And the Pi-Donor Hydrogen Bond with GLY211 at 3.19439 Å (Fig. 8).

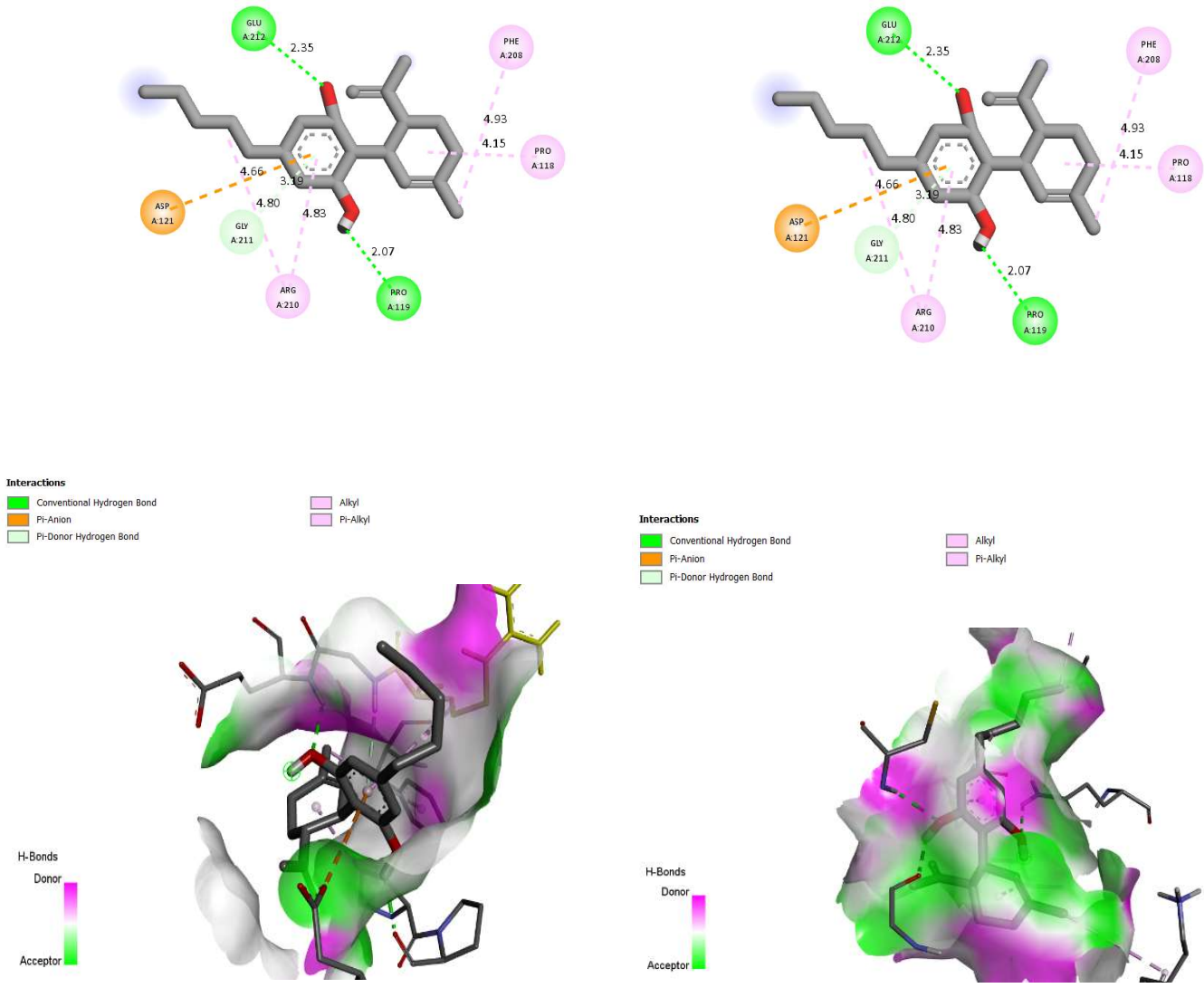

Fig. 8. 3D and 2D docked views of CBD with CB2 Protein.

Fig. 9. 3D and 2D docked views of CBD with COX-2 Protein.

Binding to COX-2. The binding affinity of CBD with COX-2 is -8.0 (kcal mol^{-1}) due to three hydrogen interactions; two created by oxygen from the hydroxyl group with (CYS1047 at 2.266 Å) and (GLN1461 at 2.543 Å) and one form by hydrogen with oxygen from the amino acid (CYS1047 at 2.266 Å). Also, CBD makes a pi bond with COX-2 according to the Pi-alkyl bond with (PRO1153 at 4.503 Å) and alkyl interactions with the following amino acids (CYS1159 at 4.580 Å), (VAL1155 at 3.715 Å), (LYS1468 at 4.800 Å), (PRO1153 at 4.481 Å), and (LEU1152 at 5.266 Å) (Fig. 9).

Binding to DR5. The binding affinity between DR5 and CBD is -8.2 (kcal mol^{-1}) because CBD makes one hydrogen bond THR68 at 2.222 Å and the hydrogen of the hydroxyl group. Also, it makes four pi-alkyl bonds with (PHE157 at 4.905 Å), (TYR181 at 4.41 Å), (TRP188 with two interactions at 5.056 Å and at 4.906 Å), and (PRO52 at 4.895Å). While four alkyl bonds are formed with (PRO52 at 4.811 Å), (ALA44 at 4.863Å), (ALA44 at 3.602 Å), (PRO52 at 4.696 Å), and (LEU123 at 3.911 Å). The Pi-Pi Stacked interaction has 4.740 Å between the benzene of CBD and that of TYR181 (Fig. 10).

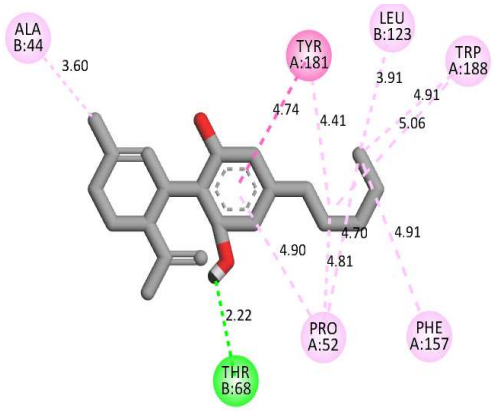

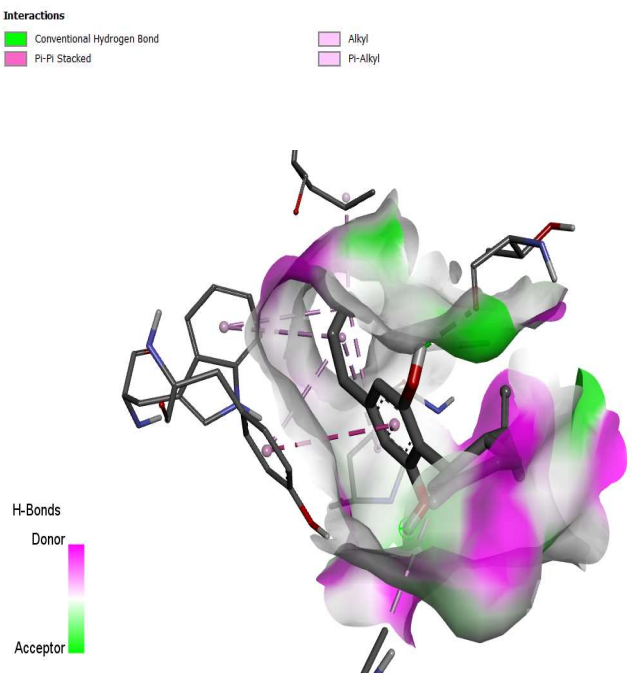

Fig. 10. 3D and 2D docked views of CBD with DR5 Protein.

Binding to EGF. The binding affinity between EGF and CBD is with EGF of -7.5 (kcal mol^{-1}) because CBD makes hydrogen bonding with (SER11 at 2.963 Å), (HIS409 at 2.241 Å), and (GLY9 at 1.99 Å). And five alkyl-type interactions with the following amino acids (LYS48 at 4.955 Å), (MET30 at 5.147 Å), (ILE38 at 5.055Å), (MET30 at 4.302 Å), and (LYS48 at 4.361 Å). Also, four pi-alkyl bonds were formed (HIS409 at 4.681 Å), (TRP49 at 5.278 Å), (TRP49 at 4.470 Å), and (ILE38 at 4.971 Å) (Fig. 11).

Binding to FAAH. The binding affinity between FAAH and CBD is -8.6 (kcal mol^{-1}) because CBD makes one Pi-Pi T-shaped interaction with (PHE432 at 5.305 Å) and four Alkyl interactions with (LEU404 at 5.141 Å), (VAL491 at 5.077 Å), (LEU404 at 3.977 Å), and (MET495 at 5.456 Å). In addition, four Pi-Alkyl bonds with (PHE432 at 4.977 Å), (PHE432 at 4.730 Å), (TRP531 at 5.054 Å), and (VAL491 at 4.380 Å) (Fig. 12).

Binding to GPR55. The binding affinity between GPR55 and CBD is -7.0 (kcal mol^{-1}) because CBD makes two hydrogen bonds (TYR308 at 2.031 Å) and (ASP128 at

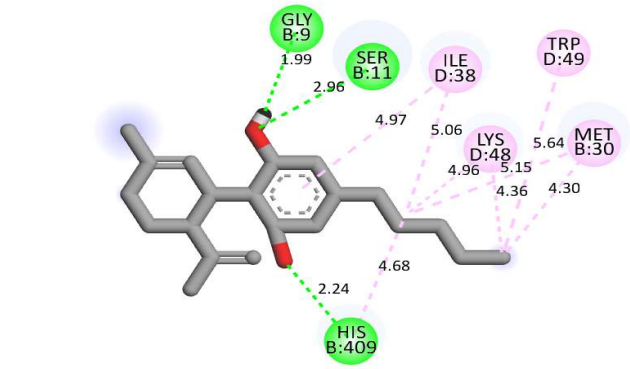

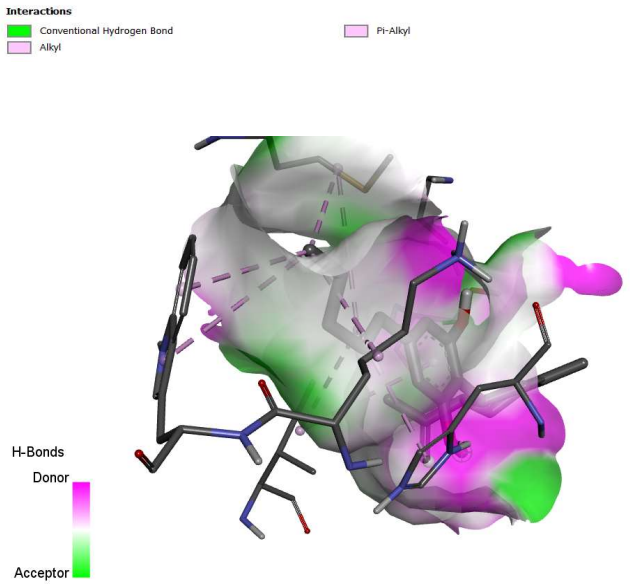

Fig. 11. 3D and 2D docked views of CBD with EGF Protein.

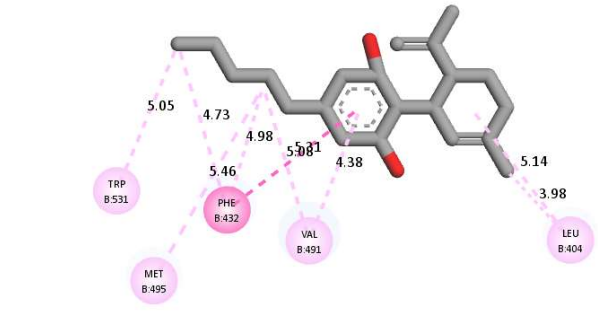

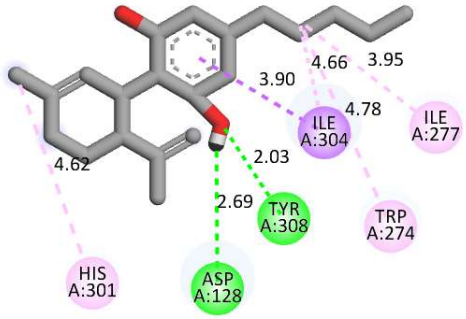

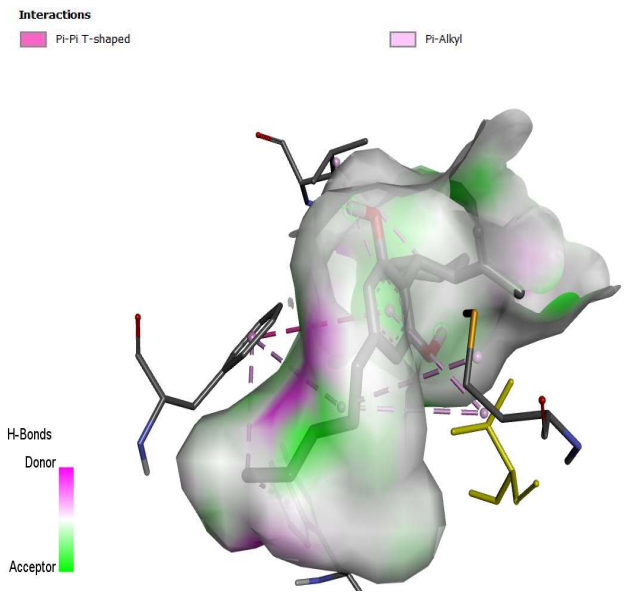

Fig. 12. 3D and 2D docked views of CBD with FAAH Protein.

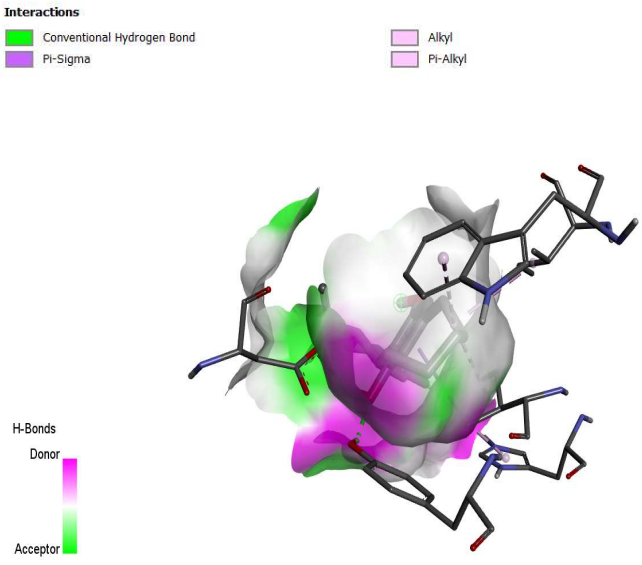

Fig. 13. 3D and 2D docked views of CBD with GPR55 Protein.

2.685 Å). One Pi-Sigma bond (ILE304 at 3.901 Å) and two Alkyl bonds with (ILE277 at 3.953 Å) and (ILE304 at 4.661 Å). And two Pi-Alkyl bonds with (TRP274 at 4.784 Å) and (HIS301 at 4.620 Å) (Fig. 13).

Binding to ICAM-1. The binding affinity between ICAM-1 and CBD is -5.2 (kcal mol^{-1}) because CBD makes one hydrogen bond (LEU94 at 2.702 Å). While a Pi-Pi T-shaped bond forms between the benzene of CBD and (TYR180 at 5.154 Å) with one alkyl bond (PRO93 at 5.119 Å) (Fig. 14).

Binding to NOS3. The binding affinity between NOS3 and CBD is -7.0 (kcal mol^{-1}) because CBD forms hydrogen bonds with NOS3 (GLY233 at 2.405 Å) and a Pi-Anion interaction at 4.01736 Å between the benzene of CBD and GLU239. In addition, two alkyl bonds exist between (CYS62 at 4.540 Å) and (ILE214 at 5.228 Å) and the carbon of CBD. Seven pi-alkyl interactions occur between the benzene groups of CBD and (PRO212 at 5.177 Å), (ILE 214 at 5.42443). The benzene rings of TRP56, PHE231, and TYR235 with the carbon of the group CBD at 5.167 Å, 5.220 Å, and 5.351 Å, respectively (Fig. 15).

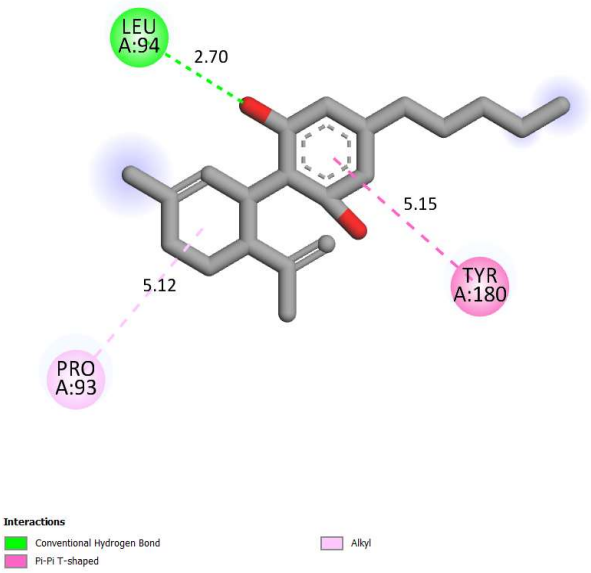

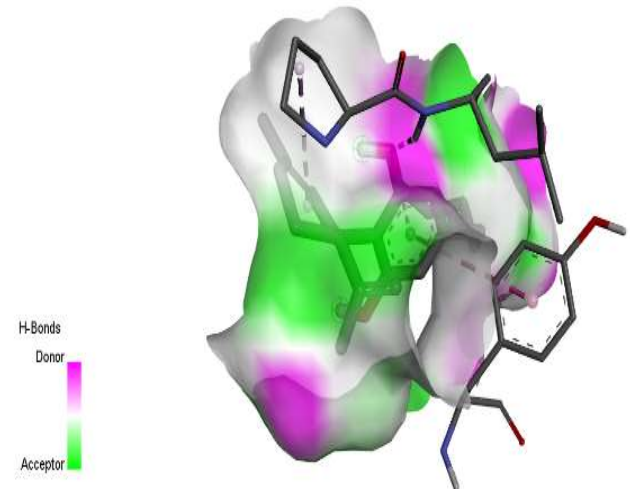

Fig. 14. 3D and 2D docked views of CBD with ICAM-1Protein.

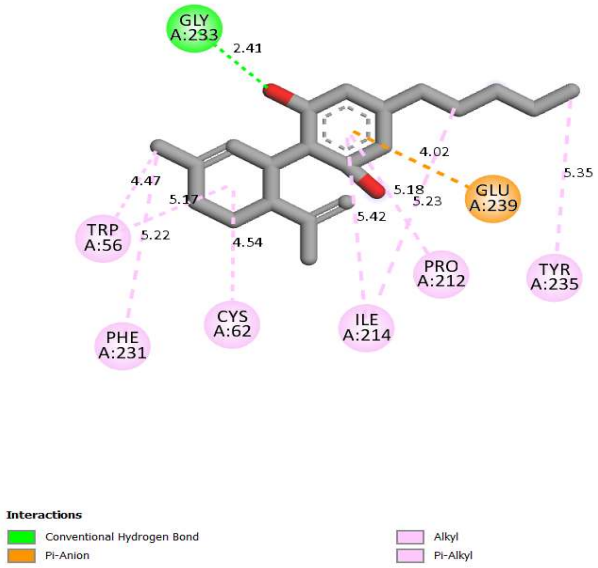

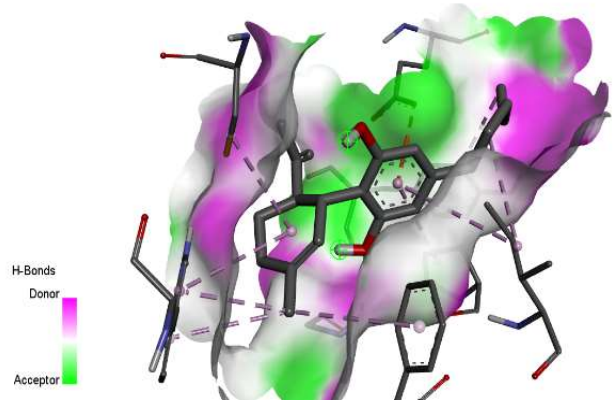

Fig. 15. 3D and 2D docked views of CBD with NOS3 Protein.

Binding to NOXA. The binding affinity between NOXA and CBD is -5.7 (kcal mol^{-1}) because CBD forms hydrogen bonds with NOXA (LYS101 has 2.496 Å). A single pi-anion was observed towards (GLU49 has 4.863 Å) and a Pi-Cation with LYS101 at 4.101 Å and Pi-Sigma with at 3.94 Å. A pi-alkyl bond with YS101 at 4.704 Å. Seven alkyl interactions with (LYS53 at 5.295 Å), (LYS101 at 5.241 Å), (ARG105 at 4.764 Å), (LYS101 at 4.322 Å), (LEU104 at 4.315 Å), (LEU56 at 4.364 Å), and (ILE98 at 5.387 Å) (Fig. 16).

Binding to PAI-1. The interaction between CBD and PAI-1 has a binding energy of -8.0 kcal mol^{-1}; CBD forms one hydrogen bond with (GLU281 at 2.281 Å) and (GLU281: O at 1.99567 Å). Also, one Pi-Sigma bond with (THR282 at 3.768 Å) and six alkyl bonds with VAL23 at 5.297 Å, VAL32 at 5.271 Å, VAL284 at 5.443 Å, LEU152 at 4.362 Å, VAL23 at 4.488 Å, and VAL284 at 4.291Å (Fig. 17).

Binding to PERK. The interaction between CBD and PERK has a binding energy of -7.0 kcal mol^{-1}. CBD forms two hydrogen bonds with ASN941 and LEU598 at 1.9138 Å

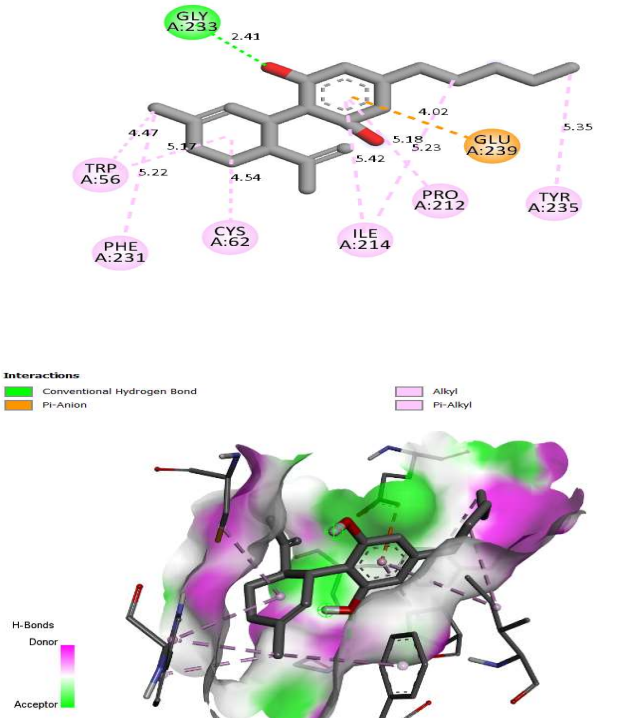

Fig. 16. 3D and 2D docked views of CBD with NOXA Protein.

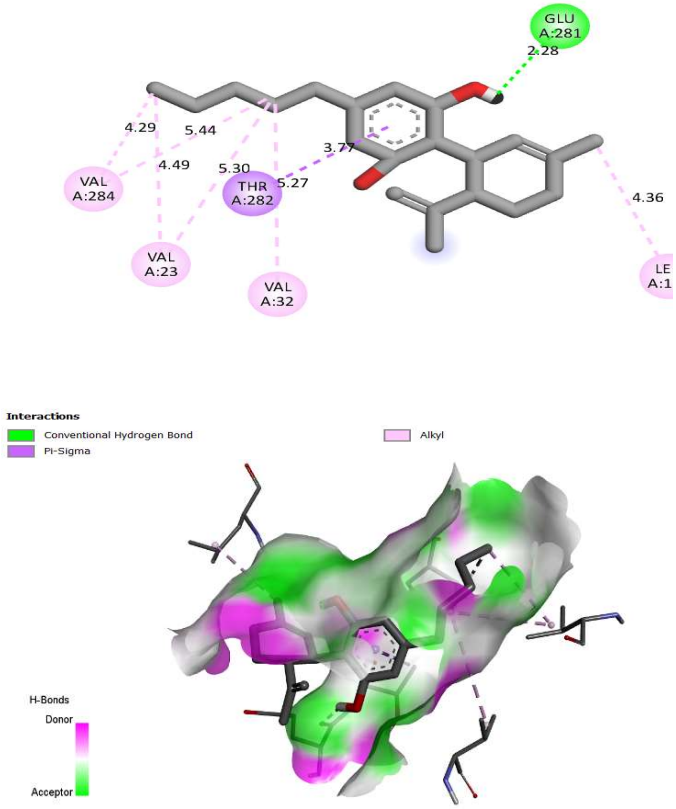

Fig. 17. 3D and 2D docked views of CBD with PAI-1 Protein.

and 2.477 Å, respectively. A pi-sigma bond with PHE943 at 3.685 Å. Also, T-shaped Pi-Pi formed with the amino acid PHE943 at 4.836 Å. in addition, two alkyl bonds (VAL606 at 4.872 Å) and (ALA619 at 4.014 Å) and two interactions (PHE943 at 5.180 Å) and (VAL606 at 4.246 Å) (Fig. 18).

Binding to PPARɣ. The interaction between CBD and PPARɣ TIMP-1 has a binding energy of -6.3 kcal mol^{-1}. It forms one carbon-hydrogen bond with GLY284 at 3.487 Å and one Pi-Sulfur interaction with MET348 at 5.129 Å. Also, four alkyl interactions with CYS285 at 4.417 Å, ARG288 at 4.606 Å, ARG280 at 3.659 Å, and ILE341at 4.749 Å. While CBD makes one pi-alkyl interaction with ILE341 at 4.497 Å (Fig. 19).

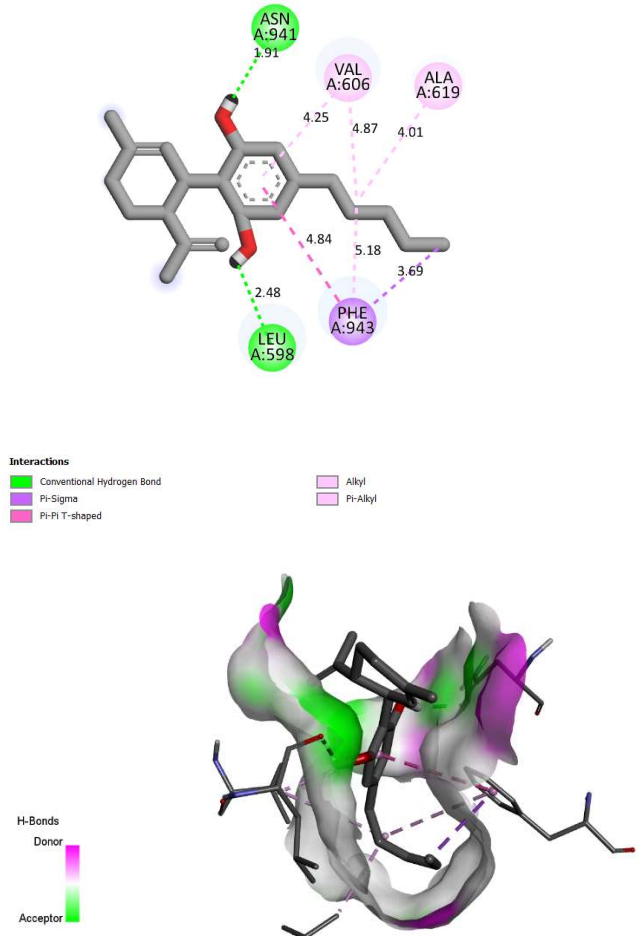

Fig. 18. 3D and 2D docked views of CBD with PERK Protein.

Binding to TIMP-1. The interaction between CBD and TIMP-1 has a binding energy of -6.7 kcal mol^{-1}. It forms one hydrogen bond with SER100 at 2.686. A Pi-Donor Hydrogen Bond interaction with VAL102 at 5.129 Å. Also. four Pi-Alkyl interactions with TYR72 at 4.108 Å and PHE101 at 3.911 Å. PRO5 at 4.248 Å and ALA103 at 4.610 Å. While CBD makes two alkyl interactions with PRO5 and ALA103 at 4.802 Å. and 4.389 Å (Fig. 20).

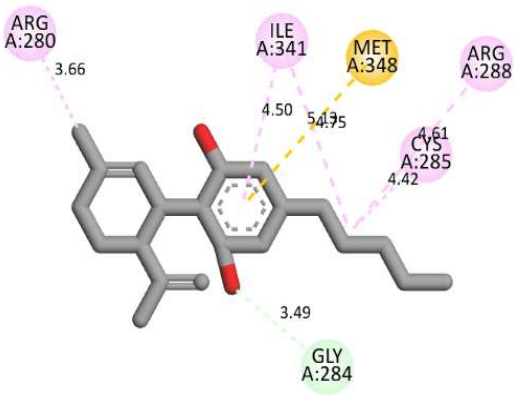

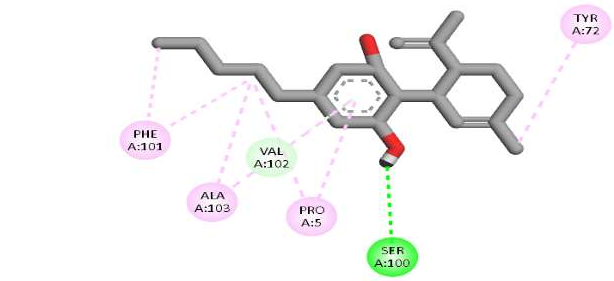

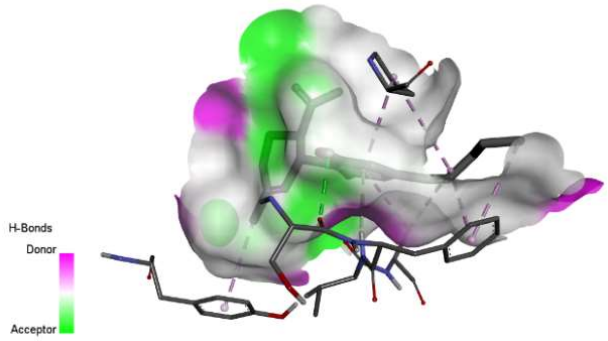

Fig. 20. 3D and 2D docked views of CBD with TIMP-1 Protein.

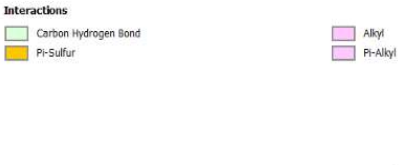

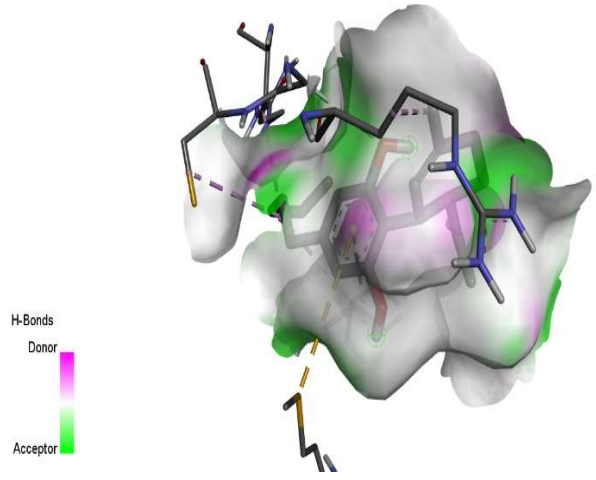

Fig. 19. 3D and 2D docked views of CBD with PPARɣ Protein.

Binding to TRV1. The interaction between CBD and TRV1 has a binding energy of -7.1 kcal mol^{-1}. It forms a conventional hydrogen bond interaction with VAL449 at 2.123 Å. A carbon-hydrogen bond with GLY479 at 3.506 Å. A Pi-Sigma interaction with THR452 and TYR456 at 3.955 Å and 3.789 Å, respectively. Two pi-alkyl with TYR456 at 4.782 Å and ALA453 at 5.061 Å. Furthermore, seven alkyl interactions (VAL449 at 4.322 Å), (ARG476 at 4.328 Å), and (ILE448 at 5.056 Å) were observed (Fig. 21).

Binding to TRV2. The interaction between CBD and TRV2 has a binding energy of -7.1 kcal mol^{-1}. It forms one conventional hydrogen bond with VAL449 at 2.123 Å. In addition, it forms three hydrophobic bonds of alkyl type (VAL449 at 4.329 Å), (ARG476 at 4.328 Å), and (4.328 at 5.056 Å). And two pi-alkyl interactions with (PHE540 at 5.43731 Å), (PHE540 at 4.54944 Å), (TYR544 at 4.10511 Å), (TYR456 at 4.782 Å), and (ALA453 at 5.061 Å). And two Pi-Sigma with (THR452 at 3.9558 Å) and (TYR456 at 3.789 Å) (Fig. 22).

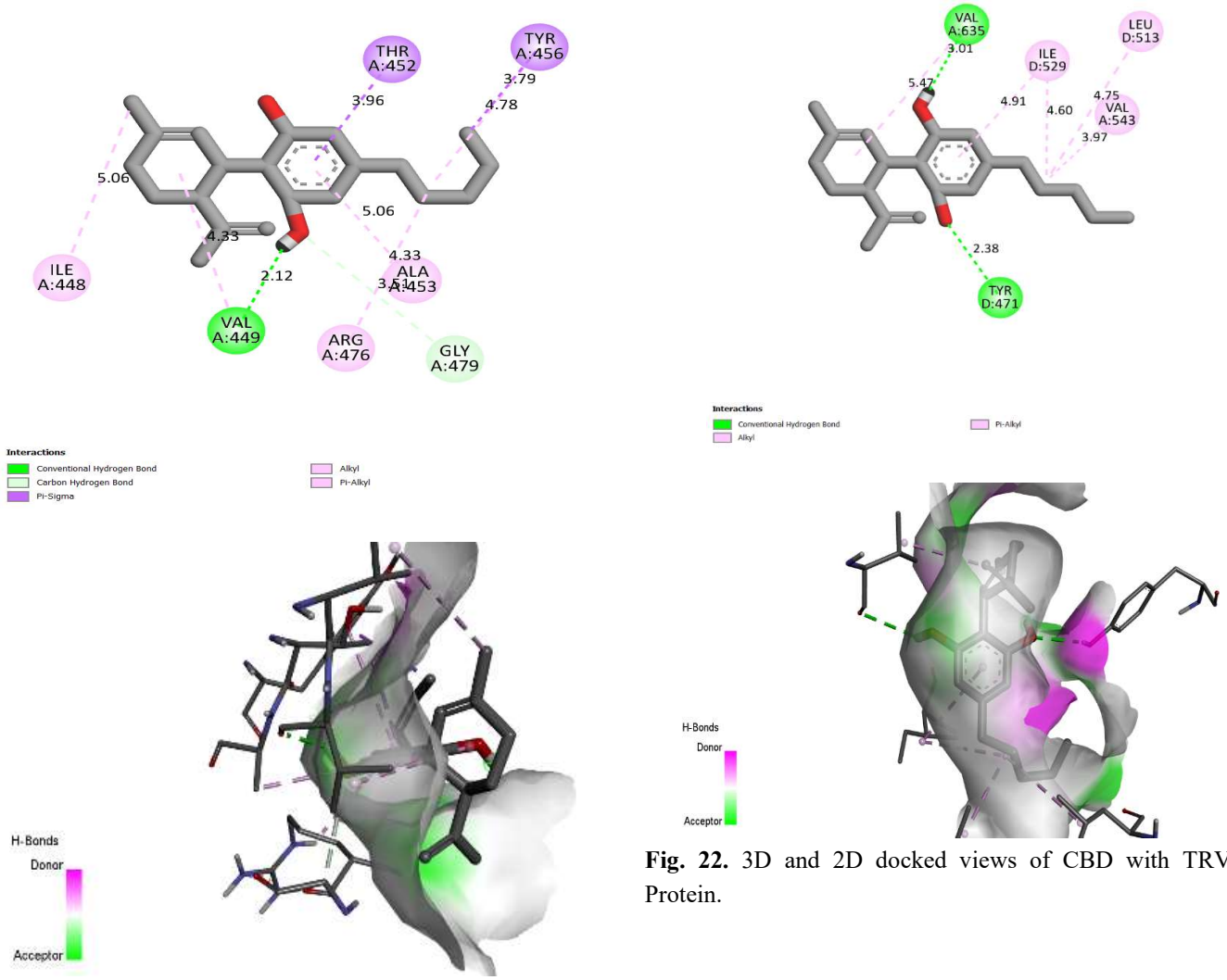

Fig. 21. 3D and 2D docked views of CBD with TRV1 Protein.

Fig. 22. 3D and 2D docked views of CBD with TRV2 Protein.

ADMET Proprieties

The ADMET properties is an acronym used in pharmacology and drug development. Standing for Absorption, Distribution, Metabolism, Excretion, and Toxicity. These properties play a crucial role in determining the pharmacokinetics and potential therapeutic value of a compound.

Table 5 presents the ADMET properties (Absorption, Distribution, Metabolism, Excretion, and Toxicity) associated with the CBD under investigation. Providing valuable insights into its potential as a drug candidate.

Based on the results obtained in Table 4. CBD absorption by the human intestine is at 90.854%. guaranteeing excellent absorption by the human intestine. However. regarding distribution indicators. the standard value of blood-brain barrier (BBB) permeability is good if its value is greater than 0.3 and poor if logBB < -1. The results show that CBD responds well to the BBB criteria which predicts that the drugs can pass through the brain. The CNS index of the compound with logPS > -2 is considered able to penetrate the CNS and the compound with logPS < -3 is considered unable to penetrate the CNS; therefore, cannabidiol can penetrate the CNS. CYP enzymes are enzymes that oxidize foreign microorganisms to facilitate their excretion. Inhibition of this enzyme can affect the drug's metabolism and the drug can have a reverse effect through 2D6 and 3A4 inhibitors responsible for drug metabolism. According to the results, CBD can be considered a substrate of CYP3A4 but not a CYP

Table 5. Results of the ADMET Test with pKCSM of CBD

Absorption	
Intestinal absorption (human)	90.854 % Absorbed
Distribution	
BBB permeability	0.181 logBB
CNS permeability	-3.911 logPS
Metabolism	
CYP 2D6 Substrate	No
CYP 3A4 Substrate	Yes
CYP 2D6 Inhibitor	No
CYP3A4 Inhibitor	No
Excretion	
Renal Oct-02 substrate	No
Toxicity	
AMES	No
Hepatoxicity	No

inhibitor. It shows that CBD's metabolism as a drug is acceptable. As for the toxicity requirement. CB has no potential harmful effect and does not cause hepatotoxicity. The analysis of the ADMET results (table 6) and the Lipinski rules (MW<=500; logP<=5; Hacc<=10; Hdon<=5) indicate that the studied molecule has been verified *in silico* as a safe pharmaceutical compound.

CONCLUSION

The results of this investigation, taken together, highlight the intriguing possibilities of cannabidiol (CBD) as a potent contender for successful tumor treatment. The energetic profile, which shows that CBD can act as an electron donor and acceptor in molecular interactions, is defined by a HOMO energy of -0.134 eV and a LUMO energy of 0.01 eV. Density Functional Theory (DFT) was utilized to conduct a thorough analysis, which demonstrated that cannabidiol's -OH groups interact through hydrogen bonding with a variety of cancer site targets. These targets include important molecules such as 5-HT1A, Becl1, COX-2, DR5, EGF, FAAH, ICAM-1, NOS3, NOXA, PAI-1, PERK, RERK, TIMP-1, and TRV1/2.

A comprehensive understanding of CBD's possible mechanisms of action in the treatment of cancer is presented by the convergence of electronic insights and molecular interaction analyses. The validation of these interactions, in addition to the values of the band gap energy (E) and negative molecular chemical potential, strengthen CBD's position as a flexible therapeutic agent.

Molecular docking simulations have revealed the resulting high binding energies, which are as follows: -8.6 kcal mol^{-1} with FAAH, -8.2 kcal mol^{-1} with DR5 and COX-2, and -8.2 kcal mol^{-1} with TRV1/2. These findings highlight the significant affinity that cannabidiol demonstrates for these particular cancer-related molecules.

These interactions point to the possibility that cannabidiol may function as a strong modulator of important cellular pathways linked to carcinogenesis. With favorable ADMET properties and strongly supported by CBD's impressive absorption rate, favorable distribution properties, and metabolic pathway that prevents major drug interactions.

Cannabidiol appears to be a promising treatment option for tumors, as indicated by the encouraging results. Though we must acknowledge the need for more thorough research, it is crucial to approach these findings with cautious optimism. To determine cannabidiol's actual effectiveness in treating cancer, thorough research is necessary. To further translate these computational insights into useful therapeutic applications, it is imperative to identify the precise molecular mechanisms underlying its anticancer activity.

Essentially, the statement advocates for a comprehensive strategy that includes both thorough empirical research to support CBD's effectiveness in treating cancer and a thorough examination of the complexities of the molecular

Table 6. Results of the Assessment of Cannabidiol (CBD) Compliance with Lipinski's Five Rules

Molecular weight (g mol^{-1})	logP	H-bond acceptors	H-bond donors	Rotatable bonds
352.773	4.28	2	2	6

structure to close the knowledge gap between theoretical understanding and useful, clinically applicable solutions. In order to successfully incorporate CBD into cancer treatment protocols and guarantee that any potential benefits are supported by solid scientific data and can be efficiently applied to patient care, a comprehensive strategy is required.

Advances in cancer treatment strategies and a deeper comprehension of the complex interactions between cannabidiol and specific cancer-related targets are two goals of ongoing research endeavors aimed at unlocking the full therapeutic potential of cannabidiol. While there is still work to be done in order to find efficient and precise tumor treatments, cannabidiol appears to be a promising contender that merits inspection and verification.

REFERENCES

[1] Brand, E. J.; Zhao, Z., Cannabis in Chinese Medicine: Are Some Traditional Indications Referenced in Ancient Literature Related to Cannabinoids? *Front. Pharmacol.* **2017**, *8*. https://doi.org/10.3389/fphar.2017.00108.

[2] Clarke, R. C.; Merlin, M. D., Letter to the Editor: Small, Ernest. 2015. Evolution and Classification of Cannabis Sativa (Marijuana, Hemp) in Relation to Human Utilization. Botanical Review *81* (3), 189-294. *Bot. Rev.* **2015**, *81* (4), 295-305. https://doi.org/10.1007/s12229-015-9158-2.

[3] Andradas, C.; Truong, A.; Byrne, J.; Endersby, R., The Role of Cannabinoids as Anticancer Agents in Pediatric Oncology. *Cancers* **2021**, *13* (1), 157. https://doi.org/10.3390/cancers13010157.

[4] Lichtor, T., *Molecular Considerations and Evolving Surgical Management Issues in the Treatment of Patients with a Brain Tumor*; BoD – Books on Demand, 2015. 436 p.

[5] Atalay, S.; Jarocka-Karpowicz, I.; Skrzydlewska, E., Antioxidative and Anti-Inflammatory Properties of Cannabidiol. *Antioxidants* **2020**, *9* (1), 21. https://doi.org/10.3390/antiox9010021.

[6] Sharafi, G.; He, H.; Nikfarjam, M., Potential Use of Cannabinoids for the Treatment of Pancreatic Cancer. *Journal of Pancreatic Cancer* **2019**, *5* (1), 1-7. https://doi.org/10.1089/pancan.2018.0019.

[7] De Almeida, D. L.; Devi, L. A., Diversity of Molecular Targets and Signaling Pathways for CBD. *Pharmacology Res & Perspec* **2020**, *8* (6), e00682. https://doi.org/10.1002/prp2.682.

[8] Jeong, S.; Yun, H. K.; Jeong, Y. A.; Jo, M. J.; Kang, S. H.; Kim, J. L.; Kim, D. Y.; Park, S. H.; Kim, B. R.; Na, Y. J.; Lee, S. I.; Kim, H. D.; Kim, D. H.; Oh, S. C.; Lee, D. -H., Cannabidiol-Induced Apoptosis Is Mediated by Activation of Noxa in Human Colorectal Cancer Cells. *Cancer Lett.* **2019**, *447*, 12-23. https://doi.org/10.1016/j.canlet.2019.01.011.

[9] Seltzer, E. S.; Watters, A. K.; MacKenzie, D.; Granat, L. M.; Zhang, D., Cannabidiol (CBD) as a Promising Anti-Cancer Drug. *Cancers* **2020**, *12* (11), E3203. https://doi.org/10.3390/cancers12113203.

[10] Kis, B.; Ifrim, F. C.; Buda, V.; Avram, S.; Pavel, I. Z.; Antal, D.; Paunescu, V.; Dehelean, C. A.; Ardelean, F.; Diaconeasa, Z.; Soica, C.; Danciu, C., Cannabidiol-from Plant to Human Body: A Promising Bioactive Molecule with Multi-Target Effects in Cancer. *Int. J. Mol. Sci.* **2019**, *20* (23), 5905. https://doi.org/10.3390/ijms20235905.

[11] Corvino, A.; Fiorino, F.; Severino, B.; Saccone, I.; Frecentese, F.; Perissutti, E.; Di Vaio, P.; Santagada, V.; Caliendo, G.; Magli, E., The Role of 5-HT1A Receptor in Cancer as a New Opportunity in Medicinal Chemistry. *Curr. Med. Chem.* **2018**, *25* (27), 3214-3227. https://doi.org/10.2174/0929867325666180209141650

[12] Ye, D.; Xu, H.; Tang, Q.; Xia, H.; Zhang, C.; Bi, F., The Role of 5-HT Metabolism in Cancer. *Biochimica et Biophysica Acta (BBA) - Reviews on Cancer* **2021**, *1876* (2), 188618. https://doi.org/10.1016/j.bbcan.2021.188618.

[13] Giatromanolaki, A.; Koukourakis, M. I.; Georgiou, I.; Kouroupi, M.; Sivridis, E. LC3A, LC3B and Beclin-1 Expression in Gastric Cancer. *Anticancer Res.* **2018**, *38* (12), 6827-6833. https://doi.org/10.21873/anticanres.13056.

[14] Khunluck, T.; Lertsuwan, K.; Chutoe, C.; Sooksawanwit, S.; Inson, I.; Teerapornpuntakit, J.; Tohtong, R.; Charoenphandhu, N., Activation of Cannabinoid Receptors in Breast Cancer Cells

Improves Osteoblast Viability in Cancer-Bone Interaction Model While Reducing Breast Cancer Cell Survival and Migration. *Sci. Rep.* **2022**, *12* (1), 7398. https://doi.org/10.1038/s41598-022-11116-9.

[15] Li, S.; Jiang, M.; Wang, L.; Yu, S. Combined Chemotherapy with Cyclooxygenase-2 (COX-2) Inhibitors in Treating Human Cancers: Recent Advancement. *Biomedicine & Pharmacotherapy* **2020**, *129*, 110389. https://doi.org/10.1016/j.biopha.2020.110389.

[16] Hou, N.; He, X.; Yang, Y.; Fu, J.; Zhang, W.; Guo, Z.; Hu, Y.; Liang, L.; Xie, W.; Xiong, H.; Wang, K.; Pang, M., TRPV1 Induced Apoptosis of Colorectal Cancer Cells by Activating Calcineurin-NFAT2-P53 Signaling Pathway. *BioMed Research International* **2019**, *2019*, 1-8. https://doi.org/10.1155/2019/6712536.

[17] Muthusami, S.; Sabanayagam, R.; Periyasamy, L.; Muruganantham, B.; Park, W. Y., A Review on the Role of Epidermal Growth Factor Signaling in the Development, Progression and Treatment of Cervical Cancer. *International Journal of Biological Macromolecules* **2022**, *194*, 179-187. https://doi.org/10.1016/j.ijbiomac.2021.11.117.

[18] Brunetti, L.; Loiodice, F.; Piemontese, L.; Tortorella, P.; Laghezza, A., New Approaches to Cancer Therapy: Combining Fatty Acid Amide Hydrolase (FAAH) Inhibition with Peroxisome Proliferator-Activated Receptors (PPARs) Activation: Miniperspective. *J. Med. Chem.* **2019**, *62* (24), 10995-11003. https://doi.org/10.1021/acs.jmedchem.9b00885.

[19] Calvillo-Robledo, A.; Cervantes-Villagrana, R. D.; Morales, P.; Marichal-Cancino, B. A., The Oncogenic Lysophosphatidylinositol (LPI)/GPR55 Signaling. *Life Sciences* **2022**, *301*, 120596. https://doi.org/10.1016/j.lfs.2022.120596.

[20] Singh, M.; Thakur, M.; Mishra, M.; Yadav, M.; Vibhuti, R.; Menon, A. M.; Nagda, G.; Dwivedi, V. P.; Dakal, T. C.; Yadav, V., (2021). Title of the article. *Immunology Letters*, *240*, 123-136. https://doi.org/10.1016/j.imlet.2021.10.007

[21] Luo, L.; Xia, L.; Zha, B.; Zuo, C.; Deng, D.; Chen, M.; Hu, L.; He, Y.; Dai, F.; Wu, J.; Wang, C.; Wang, Y.; Zhang, Q., (2018). miR-335-5p targeting ICAM-1 inhibits invasion and metastasis of thyroid cancer cells. *Biomedicine & Pharmacotherapy*, *106*, 983-990. https://doi.org/10.1016/j.biopha.2018.07.046.

[22] Jeong, S.; Kim, B. G.; Kim, D. Y.; Kim, B. R.; Kim, J. L.; Park, S. H.; Na, Y. J.; Jo, M. J.; Yun, H. K.; Jeong, Y. A.; Kim, H. J.; Lee, S. I.; Kim, H. D.; Kim, D. H.; Oh, S. C.; Lee, D. -H., Cannabidiol Overcomes Oxaliplatin Resistance by Enhancing NOS3- and SOD2-Induced Autophagy in Human Colorectal Cancer Cells. *Cancers* **2019**, *11* (6), 781. https://doi.org/10.3390/cancers11060781.

[23] Jeong, S.; Yun, H. K.; Jeong, Y. A.; Jo, M. J.; Kang, S. H.; Kim, J. L.; Kim, D. Y.; Park, S. H.; Kim, B. R.; Na, Y. J.; Lee, S. I.; Kim, H. D.; Kim, D. H.; Oh, S. C.; Lee, D. -H., (2019). Cannabidiol-induced apoptosis is mediated by activation of Noxa in human colorectal cancer cells. *Cancer Lett.*, *447*, 12-23. https://doi.org/10.1016/j.canlet.2019.01.011

[24] Drozd, M.; Marzęda, P.; Czarnota, J.; Dobrzyński, M.; Skubel, T.; Dudek, I.; Rybak, N., The Potential of Cannabinoids in the Treatment of Lung Cancer. *J. Educ. Health Sport* **2022**, *12* (8), 1100-1110. https://doi.org/10.12775/JEHS.2022.12.08.094.

[25] Fan, P.; Jordan, V. C., PERK, Beyond an Unfolded Protein Response Sensor in Estrogen-Induced Apoptosis in Endocrine-Resistant Breast Cancer. *Mol. Cancer Res.* **2022**, *20* (2), 193-201. https://doi.org/10.1158/1541-7786.MCR-21-0702.

[26] Liu, S.; Shi, J.; Wang, L.; Huang, Y.; Zhao, B.; Ding, H.; Liu, Y.; Wang, W.; Chen, Z.; Yang, J., Loss of EMP1 Promotes the Metastasis of Human Bladder Cancer Cells by Promoting Migration and Conferring Resistance to Ferroptosis through Activation of PPAR Gamma Signaling. *Free Radical Biology and Medicine* **2022**, *189*, 42-57. https://doi.org/10.1016/j.freeradbiomed.2022.06.247.

[27] He, X.; Shi, L.; Qiu, M.; Li, Q.; Wang, M.; Xiong, Z.; Yang, S., Molecularly Targeted Anti-Cancer Drugs Inhibit the Invasion and Metastasis of Hepatocellular Carcinoma by Regulating the Expression of MMP and TIMP Gene Families. *Biochemical and Biophysical Research Communications* **2018**, *504* (4), 878-884. https://doi.org/10.1016/j.bbrc.2018.08.203.

[28] Hou, N.; He, X.; Yang, Y.; Fu, J.; Zhang, W.; Guo, Z.; Hu, Y.; Liang, L.; Xie, W.; Xiong, H.; Wang, K.; Pang,

M., TRPV1 Induced Apoptosis of Colorectal Cancer Cells by Activating Calcineurin-NFAT2-P53 Signaling Pathway. *BioMed Res. Int.* **2019**, *2019*, e6712536. https://doi.org/10.1155/2019/6712536.

[29] Marinelli, O.; Morelli, M. B.; Annibali, D.; Aguzzi, C.; Zeppa, L.; Tuyaerts, S.; Amantini, C.; Amant, F.; Ferretti, B.; Maggi, F.; Santoni, G.; Nabissi, M, The Effects of Cannabidiol and Prognostic Role of TRPV2 in Human Endometrial Cancer. *Int. J. Mol. Sci.* **2020**, *21* (15), 5409. https://doi.org/10.3390/ijms21155409.

[30] Heider, C. G.; Itenberg, S. A.; Rao, J.; Ma, H.; Wu, X., Mechanisms of Cannabidiol (CBD) in Cancer Treatment: A Review. *Biology (Basel)* **2022**, *11* (6), 817. https://doi.org/10.3390/biology11060817.

[31] Massi, P.; Solinas, M.; Cinquina, V.; Parolaro, D., Cannabidiol as Potential Anticancer Drug. *Br J. Clin. Pharmacol* **2013**, *75* (2), 303-312. https://doi.org/10.1111/j.1365-2125.2012.04298.x.

[32] Hajji, H.; Tabti, K.; En-nahli, F.; Bouamrane, S.; Lakhlifi, T.; Ajana, M.; Bouachrine, M., *In Silico* Investigation on the Beneficial Effects of Medicinal Plants on Diabetes and Obesity: Molecular Docking, Molecular Dynamic Simulations, and ADMET Studies. *Biointerface Res. Appl. Chem.* **2021**, *11*, 6933-6949. https://doi.org/10.33263/BRIAC115.69336949.

[33] Tabti, K.; Hajji, H.; Sbai, A.; Maghat, H.; Bouachrine, M.; Lakhlifi, T., Identification of a Potential Thiazole Inhibitor Against Biofilms by 3D QSAR, Molecular Docking, DFT Analysis, MM-PBSA Binding Energy Calculations, and Molecular Dynamics Simulation. *Phys. Chem. Res.* **2023**, 369-389. https://doi.org/10.22036/pcr.2022.335657.2068.

[34] Trott, O.; Olson, A. J., AutoDock Vina: Improving the Speed and Accuracy of Docking with a New Scoring Function, Efficient Optimization, and Multithreading. *J. Comput. Chem.* **2010**, *31* (2), 455-461. https://doi.org/10.1002/jcc.21334.

[35] Fukui, K., Role of Frontier Orbitals in Chemical Reactions. *Science* **1982**, *218* (4574), 747-754. https://doi.org/10.1126/science.218.4574.747.

[36] Adjissi, L.; Chafai, N.; Benbouguerra, K.; Kirouani, I.; Hellal, A.; Layaida, H.; Elkolli, M.; Bensouici, C.; Chafaa, S., Synthesis, Characterization, DFT, Antioxidant, Antibacterial, Pharmacokinetics and Inhibition of SARS-CoV-2 Main Protease of Some Heterocyclic Hydrazones. *J. Mol. Struct.* **2022**, *1270*, 134005. https://doi.org/10.1016/j.molstruc.2022.134005.

[37] De Vleeschouwer, F.; Van Speybroeck, V.; Waroquier, M.; Geerlings, P.; De Proft, F., Electrophilicity and Nucleophilicity Index for Radicals. *Org. Lett.* **2007**, *9* (14), 2721-2724. https://doi.org/10.1021/ol071038k.

[38] Selvaraj, S.; Ram Kumar, A.; Ahilan, T.; Kesavan, M.; Serdaroglu, G.; Rajkumar, P.; Mani, M.; Gunasekaran, S.; Kumaresan, S., Experimental and Theoretical Spectroscopic Studies of the Electronic Structure of 2-Ethyl-2-phenylmalonamide. *Phys. Chem. Re*s, **2022**, *10* (3), 333-344, DOI: 10.22036/ PCR.2021.304087.1966.

[39] Ram Kumar, A.; Selvaraj, S.; Kanagathara, N., Spectroscopic, Structural and Molecular Docking Studies on N,N-Dimethyl-2-[6-methyl-2-(4-methylphenyl) Imidazo [1,2-a] pyridin-3-yl] Acetamide*, Phys. Chem. Res*. **2024**, *12*, 95-107, DOI: 10.22036/PCR.2023.387911.2306.

[40] The Theoretical Prediction of Thermophysical Properties, HOMO, LUMO, QSAR and Biological Indics of Cannabinoids (CBD) and Tetrahhdrocannabinol (THC) by Computational Chemistry. *Adv. J. Chem. A* **2019**, *2* (3), 190-202. https://doi.org/10.33945/SAMI/AJCA.2019.2.190202.

[41] Leboeuf, M.; Köster, A. M.; Jug, K.; Salahub, D. R., Topological Analysis of the Molecular Electrostatic Potential. *J. Chem. Phys.* **1999**, *111* (11), 4893-4905. https://doi.org/10.1063/1.479749.

[42] Lakshminarayanan, S.; Jeyasingh, V.; Murugesan, K.; Selvapalam, N.; Dass, G., Molecular Electrostatic Potential (MEP) Surface Analysis of Chemo Sensors: An Extra Supporting Hand for Strength, Selectivity & Non-Traditional Interactions. *Journal of Photochemistry and Photobiology* **2021**, *6*, 100022. https://doi.org/10.1016/j.jpap.2021.100022.

[43] Toprak, Ş., (2021). Theoretical calculation of some chemical properties of the cannabidiol (CBD) molecule. *International Journal of Science and Literature*, *3* (2), 129-142. https://doi.org/10.38058/ijsl.982145.